Fermi National Accelerator Laboratory

FERMILAB– Conf-88/76-T
June 1988

Renormalization Effects on Phenomenological Mass Matrices Illustrated for the Fritzsch Model

CARL H. ALBRIGHT*
and
MANFRED LINDNER

Fermi National Accelerator Lab.
P.O. Box 500, Batavia, IL 60510 (USA)

ABSTRACT

In view of the important nonlinear contributions to the renormalization group equations for the Yukawa coupling matrices, the naive application of unrenormalized models to low energy data is rather questionable. Here we investigate the renormalization effects for the specific case of the Fritzsch model. We show how the comparison with experimental data on the KM matrix elements and $B - \bar{B}$ mixing, in particular, is modified.

Permanent address: Department of Physics, Northern Illinois University, DeKalb, Illinois 60115

Operated by Universities Research Association Inc. under contract with the United States Department of Energy

Most predictions for the structure of quark mass matrices have their origin in a hypothetical contact with an underlying model. It is the matching of degrees of freedom at a scale where this contact occurs that determines the structure. In many scenarios the typical scales of contact are very high, so that the renormalization of the ansatz becomes potentially important when compared with low energy data. If, however, all renormalization effects are universal in generation space, i.e., proportional to the unit matrix; then a universal rescaling of the spectrum is the only effect. Since typically only the relative spectrum is explained by phenomenological mass matrices, this rescaling can be absorbed and the unrenormalized ansatz can be used for the low energy spectrum and mixings. This universality in flavor space also guaranties that the Kobayashi–Maskawa mixing matrix [1] is not affected by renormalization. Once rotated in a certain basis, the ansatz will remain in this basis up to overall normalization factors.

The picture changes when nonuniversal renormalization effects are present. The initial structure will start to change, since there is no symmetry within the standard model (or whatever extension is assumed) which protects it. The changes will in general be both physical and unphysical: part of the changes can be transformed away by righthanded rotations on the fields, but lefthanded rotations and relative changes in the spectrum of eigenvalues will be physically significant.

We shall demonstrate here that changes in the KM mixing matrix show up earlier than changes in the relative spectrum. Two reasons for this are the high precision to which some KM matrix elements are known and the strong correlations in the changes of the elements. To be specific, we let the three generation standard model be valid up to a scale of 10^5 GeV where a phenomenological ansatz of the Fritzsch type [2] is assumed. Elsewhere [3] we shall generalize the results to the 2-Higgs and supersymmetric standard models.

The renormalization group equations for the mass matrices are given by [4]

$$-16\pi^2\frac{dM_Y}{dt} = \left(G_Y\ \mathbf{1} - T_Y\ \mathbf{1} - \frac{3}{2}S_Y\right)M_Y\ , \quad Y = U,\ D \ \text{ for up and down} \tag{1}$$

where

$$t = ln\left(\frac{\mu}{1\ GeV}\right)\ , \qquad M_Y = \frac{m_Y}{v}\ , \qquad v \simeq 175\ GeV$$

$$G_U = 8g_3^2 + \frac{9}{4}g_2^2 + \frac{17}{12}g_1^2\ , \qquad G_D = 8g_3^2 + \frac{9}{4}g_2^2 + \frac{5}{12}g_1^2$$

$$T_U = T_D = 3\ Trace\left(M_U M_U^+ + M_D M_D^+\right)$$

$$S_U = -S_D = M_U M_U^+ - M_D M_D^+$$

We can see immediately that the G_Y and T_Y terms are universal in generation space and result in universal rescaling factors r which can be absorbed in a structural ansatz. The absolute magnitude of the spectrum will not be explained here; therefore, we can drop these factors r, since they do not change anything in the mixing matrix or relative spectrum.

The evolution of the mixing angles has been solved in [4] to a very good approximation for three generations in the original KM parametrization:

$$\begin{array}{rclr} \theta_1(t) & = & \bar{\theta}_1 & +\mathbf{O}(\theta^3) \\ \theta_{23}(t) & = & \bar{\theta}_{2,3}\beta^{\frac{1}{2}} & +\mathbf{O}(\theta^3)\ , \\ \delta(t) & = & \bar{\delta} & +\mathbf{O}(\theta^3) \end{array} \tag{2}$$

where the bar always denotes quantities at $\mu = 1\ GeV$ ($t = 0$) with

$$\beta(t) = exp\left(\frac{3}{16\pi^2}\int_0^t g_{top}^2\ d\tau\right) \simeq exp\left[\frac{3}{16\pi^2}\frac{m_t^2}{v^2}ln\left(\frac{\mu}{1\ GeV}\right)\right] \tag{3}$$

Our numerical results will refer to $10^5\ GeV$ which puts β in the range between 1.0 and 1.25. Expanding U_{KM} in small quantities we find

$$U_{KM}(t) = \begin{pmatrix} \bar{U}_{11} & \bar{U}_{12} & \bar{U}_{13}\beta^{\frac{1}{2}} \\ \bar{U}_{21} & \bar{U}_{22} - \frac{1}{2}\bar{U}_{23}(\beta^{\frac{1}{2}} - 1) & \bar{U}_{23}\beta^{\frac{1}{2}} \\ \bar{U}_{31}\beta^{\frac{1}{2}} & \bar{U}_{32}\beta^{\frac{1}{2}} & \bar{U}_{33} - \frac{1}{2}\bar{U}_{23}(\beta^{\frac{1}{2}} - 1) \end{pmatrix} \tag{4}$$

expressed in terms of $\bar{U}_{ij} = (U_{KM})_{ij}(0)$. The relative spectral changes can also be extracted from [4]:

$$\begin{array}{lll} m_u(t) = r_u\bar{m}_u\ , & m_c(t) = r_u\bar{m}_c\ , & m_t(t) = r_u\bar{m}_t\beta^{\ \frac{1}{2}} \\ m_d(t) = r_d\bar{m}_d\ , & m_s(t) = r_d\bar{m}_s\ , & m_b(t) = r_d\bar{m}_b\beta^{-\frac{1}{2}} \end{array} \tag{5}$$

The overall rescalings r_u and r_d will cancel later on as expected, and only m_b and m_t get slightly changed in the relative spectrum by powers of β. The bar again denotes quantities defined at $\mu = 1\ GeV$.

Equations (4) and (5) allow us to discuss the matching of low energy data to a specific ansatz at a higher scale. A given set of low energy masses and KM matrix elements (including errors) has to be transformed to the relevant scale by (4) and (5). All scale dependencies enter via β, a quantity which will aproach unity if the scale difference vanishes. Later on we will use masses evolved to the scale where a special ansatz holds as input to find the predictions for the evolved KM matrix elements.

We shall use the mixings determined at 1 GeV by Schubert [5] :

$$|\bar{U}_{KM}|^2 = \begin{pmatrix} .9506 - .9522 & .04787 - .04946 & (0 - 1.5138)10^{-4} \\ .04770 - .04937 & .9483 - .9502 & (.1600 - .2704)10^{-2} \\ (.0225 - 4.219)10^{-4} & (.1498 - .2615)10^{-2} & .9972 - .9984 \end{pmatrix} \tag{6}$$

Later on we shall find in lowest order that all mixings depend on just four independent mass ratios. From Ref. 6 we find for these ratios at 1 GeV:

$$\begin{aligned} \epsilon_{12} &= \frac{\bar{m}_u}{\bar{m}_c} = 0.0039 \pm 0.0011, & \epsilon_{23} &= \frac{\bar{m}_c}{\bar{m}_t} \leq 0.023 \\ \tilde{\epsilon}_{12} &= \frac{\bar{m}_d}{\bar{m}_s} = 0.051 \pm 0.004, & \tilde{\epsilon}_{23} &= \frac{\bar{m}_s}{\bar{m}_b} = 0.033 \pm 0.011 \end{aligned} \tag{7}$$

Note that ratios of light quarks (u,d,s) are known rather precisely from current algebra, while ratios of heavy quarks (c,b,t) are also well determined. But ratios involving a light and a heavy quark, ϵ_{12} and $\tilde{\epsilon}_{23}$, are known rather poorly. Hence they will later spoil rather precise predictions.

For purposes of illustration we combine the above mass and mixing evolutions with the specific Fritzsch ansatz [2] at a high symmetry-breaking scale, where the mass matrices assume the particularly simple form

$$M_Y = \begin{pmatrix} 0 & A_Y e^{i\varphi_{A_Y}} & 0 \\ A_Y e^{-i\varphi_{A_Y}} & 0 & B_Y e^{i\varphi_{B_Y}} \\ 0 & B_Y e^{-i\varphi_{B_Y}} & C_Y \end{pmatrix} \tag{8}$$

with A_Y , B_Y, $C_Y \in \mathbf{R}^+$, and Y is again U for up quarks or D for down quarks. Due to the S_Y terms in (1), the predictions will depend on the scale where the ansatz is imposed. The product $M_Y M_Y^+$ is, in general, diagonalized by a unitary transformation X_Y:

$$X_Y M_Y M_Y^+ X_Y^+ = diag(m_1^2, m_2^2, m_3^2) \tag{9}$$

Note that $\lambda_1 = m_1$, $\lambda_2 = -m_2$, $\lambda_3 = m_3$ ($m_i > 0$) is used as usual for the eigenvalues of (8) to obtain $|\lambda_1| < |\lambda_2| < |\lambda_3|$. The parameters A, B, C will be expressed in terms of masses m_1, m_2, m_2, via relations coming from the characteristic equation, because ultimately we want to use phenomenological masses as input to predict the KM mixings. Therefore X_Y can be expressed entirely in terms of masses and free phases. We observe that the result for each X_Y depends only on two independent quark mass ratios involving different generations, i.e., $\frac{m_1}{m_2}$ and $\frac{m_2}{m_3}$, which are both small numbers. The exact results for the absolute squares of the KM matrix elements, as determined directly from $U = X_U X_D^+$ or with the invariant function technique of Jarlskog [7], can therefore be expanded in terms of these mass ratios, and we find in leading order

$$
\begin{aligned}
|U_{11}|^2 &\simeq 1 - \tfrac{m_u}{m_c} - \tfrac{m_d}{m_s} + 2\sqrt{\tfrac{m_u}{m_c}\tfrac{m_d}{m_s}}\, cos\Phi_A \\
|U_{12}|^2 &\simeq \tfrac{m_u}{m_c} + \tfrac{m_d}{m_s} - 2\sqrt{\tfrac{m_u}{m_c}\tfrac{m_d}{m_s}}\, cos\Phi_A \\
|U_{13}|^2 &\simeq \tfrac{m_u}{m_c}\left(\tfrac{m_s}{m_b} + \tfrac{m_c}{m_t} - 2\sqrt{\tfrac{m_s}{m_b}\tfrac{m_c}{m_t}}\, cos\Phi_B\right) \\
|U_{21}|^2 &\simeq \tfrac{m_u}{m_c} + \tfrac{m_d}{m_s} - 2\sqrt{\tfrac{m_u}{m_c}\tfrac{m_d}{m_s}}\, cos\Phi_A \\
|U_{22}|^2 &\simeq 1 - \tfrac{m_u}{m_c} - \tfrac{m_c}{m_t} - \tfrac{m_d}{m_s} - \tfrac{m_s}{m_b} + 2\left(\sqrt{\tfrac{m_u}{m_c}\tfrac{m_d}{m_s}}\, cos\Phi_A + \sqrt{\tfrac{m_c}{m_t}\tfrac{m_s}{m_b}}\, cos\Phi_B\right) \\
|U_{23}|^2 &\simeq \tfrac{m_s}{m_b} + \tfrac{m_c}{m_t} - 2\sqrt{\tfrac{m_s}{m_b}\tfrac{m_c}{m_t}}\, cos\Phi_B \\
|U_{31}|^2 &\simeq \tfrac{m_d}{m_s}\left(\tfrac{m_s}{m_b} + \tfrac{m_c}{m_t} - 2\sqrt{\tfrac{m_s}{m_b}\tfrac{m_c}{m_t}}\, cos\Phi_B\right) \\
|U_{32}|^2 &\simeq \tfrac{m_s}{m_b} + \tfrac{m_c}{m_t} - 2\sqrt{\tfrac{m_s}{m_b}\tfrac{m_c}{m_t}}\, cos\Phi_B \\
|U_{33}|^2 &\simeq 1 - \tfrac{m_c}{m_t} - \tfrac{m_s}{m_b} + 2\sqrt{\tfrac{m_c}{m_t}\tfrac{m_s}{m_b}}\, cos\Phi_B
\end{aligned}
\tag{10}
$$

Given the numerical size of the epsilon mass ratios in (7), we observe that the second order terms are of the order of the errors of the data in (6). But the approximations in (10) are sufficient to give us a simple understanding of the allowed parameter space and, more importantly, enable us to see whether the leading contributions are renormalized and, if so, what changes occur. In a hypothetical expansion of $|U_{KM}|^2$ to sufficiently high precision, the changes due to renormalization would be given to a very good approximation by the alterations of the first terms affected by renormalization. So even if the expansion (10) is not sufficient for comparison with data, we can still extract the changes due to renormalization fairly accurately. A more detailed treatment of the renormalization effects will be treated elsewhere [3].

To understand the allowed parameter range, it is important to realize that, of all the available information, the experimental bounds on $|U_{12}|^2$ and $|U_{23}|^2$ impose the strongest constraints on the Fritzsch model parameters. The two relations for $|U_{12}|^2$ and $|U_{23}|^2$ in (10) have simple geometrical interpretations in terms of the two triangles shown in Fig. 1, where one side corresponds to the magnitude of a KM matrix element and the other two sides are just square roots of appropriate quark mass ratios.

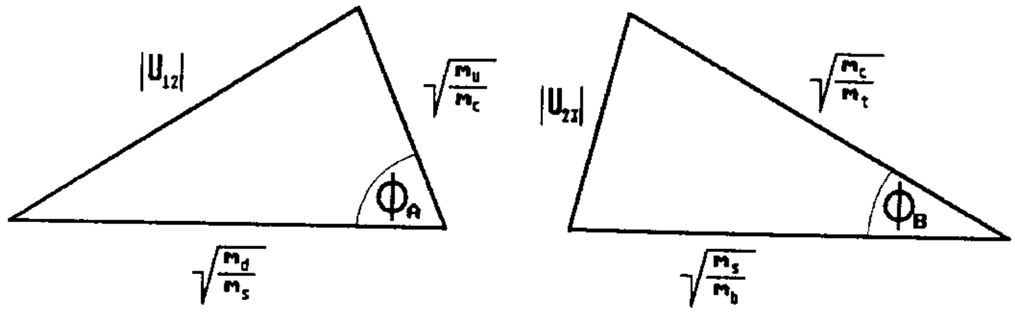

Fig. 1. Triangles involving U_{12} and U_{23}.

The triangle inequality for $|U_{12}|^2$ reads

$$\left(\sqrt{\frac{m_u}{m_c}}-\sqrt{\frac{m_d}{m_s}}\right)^2 \leq |U_{12}|^2 \leq \left(\sqrt{\frac{m_u}{m_c}}+\sqrt{\frac{m_d}{m_s}}\right)^2 \tag{11}$$

and since it involves just first and second generation quark masses, we see from (5) that it is invariant with respect to the renormalization effects in first order. The inequalities are satisfied for the Gasser-Leutwyler quark masses of Ref. 6, so we can solve for $cos\Phi_A$ and find

$$cos\Phi_A = \frac{\frac{m_u}{m_c}+\frac{m_d}{m_s}-|U_{12}|^2}{2\sqrt{\frac{m_u}{m_c}}\sqrt{\frac{m_d}{m_s}}} = \frac{\epsilon_{12}+\bar{\epsilon}_{12}-|U_{12}|^2}{2\sqrt{\epsilon_{12}\bar{\epsilon}_{12}}} \tag{12}$$

at both the high symmetry-breaking scale and 1 GeV scale. Varying all input data give $\Phi_A = 78^o \pm 3^o$, independent of the top quark mass. Comparison with numerical simulations for which $\Phi_A = 84^o \pm 3^o$ shows that the results are good, but not precise enough to compare with the experimental errors. The near cancellation in the numerator implies that second-order corrections should actually be taken into account here.

The second relevant constraint comes from the triangle inequality for $|U_{23}|^2$. Again, when

$$\left(\sqrt{\frac{m_c}{m_t}}-\sqrt{\frac{m_s}{m_b}}\right)^2 \leq |U_{23}|^2 \leq \left(\sqrt{\frac{m_c}{m_t}}+\sqrt{\frac{m_s}{m_b}}\right)^2 \tag{13}$$

is fulfilled, we can solve for $cos\Phi_B$ and find

$$cos\Phi_B = \frac{\frac{m_c}{m_t}+\frac{m_s}{m_b}-|U_{23}|^2}{2\sqrt{\frac{m_c}{m_t}}\sqrt{\frac{m_s}{m_b}}} = \frac{\beta^{-1/2}\epsilon_{23}+\beta^{1/2}\bar{\epsilon}_{23}-|U_{23}|^2}{2\sqrt{\epsilon_{23}\bar{\epsilon}_{23}}} \tag{14}$$

This time the solution will, if it exists, depend on the top mass; moreover, it is renormalization-dependent. Since $\frac{m_s}{m_b}$ is much larger than $|U_{23}|^2$, it is clear from

(14) and the left hand side of (13) that only for $\frac{m_c}{m_t} \simeq \frac{m_s}{m_b}$ can solutions exist and then only for Φ_B small. For small Φ_B, we expect a stable result, so the first order terms should give fairly accurate results here.

In Fig. 2a we use the geometrical construction of Fig. 1 to find the allowed parameter range of (14) with evolution ignored. In Fig. 2b the same data are plotted in the $\Phi_B - m_t$ plane which nicely reproduces the earlier results of Ref. 8. To include renormalization effects we just need to replace the masses and mixings by running quantities as in (14). All rescaling factors r cancel as expected and only ratios of second and third generation quarks together with $|U_{23}|$ get corrected.

The most important issue is the allowed range of top quark masses which is given in (14) for $\Phi_B = 0$ by

$$\sqrt{\frac{m_c}{m_t}} - \sqrt{\frac{m_s}{m_b}} = \pm|U_{23}| \tag{15}$$

or after inserting evolved masses

$$(\bar{m}_t)_{\frac{min}{max}} = \frac{\bar{m}_c}{\beta\left(\sqrt{\frac{\bar{m}_s}{\bar{m}_b}} \pm |\bar{U}_{23}|\beta^{\frac{1}{4}}\right)^2} \tag{16}$$

Note that these equations are selfconsistency equations since β is a function of $\bar{m}_t$. We start using $\bar{m}_t = 0$ for β on the right hand side and calculate a top mass which will be input for the next itteration until the result is reasonably stable. The lower end of the allowed range is more or less not changed by renormalization effects since β is very close to unity for such top masses. The upper end of the allowed range is a balance of different corrections in (16). Since $|U_{23}|^2 \ll \frac{\bar{m}_s}{\bar{m}_b}$ most of the effect is given by the β^{-1} factor in (16) which reduces the upper end of the allowed range by about 10% for a high scale of $10^5\ GeV$.

Additional important experimental information constraining the top quark mass and restricting the validity of the Fritzsch model comes from the recent ARGUS results [9] on $B_d - \bar{B}_d$ mixing. In the previous analysis of Ref. 8 which ignored non-linear renormalization effects, it was found that the KM-allowed region for the top mass did not overlap the $B - \bar{B}$ mixing band as shown in Fig. 2b for the Fritzsch ansatz applied to the standard model. Hence it is of interest to see if inclusion of the nonlinear renormalization effects changes the situation.

It is customary to approximate $x_d \equiv \Delta m_{B_L - B_S}/\Gamma_B$ by the one-loop box diagram involving just W boson exchange in the standard model. As shown in [8], the equation of interest can be expressed as

$$m_t^2|U_{33}U_{31}^*|^2 R \simeq (2.0 \pm 0.5)\frac{(0.140)^2}{B_B f_B^2} \tag{17}$$

in terms of the ARGUS results. The parameter R is slowly varying and nearly renormalization-independent, while the running mass and the KM matrix elements should be evaluated near the W or Z mass. The combination of interest which appears on the lefthand side of (17) is seen to evolve according to

$$m_t^2|U_{33}U_{31}^*|^2 \simeq r_u^2\beta^2\bar{m}_t^2|\bar{U}_{33}\bar{U}_{31}^*|^2 \tag{18}$$

which receives a scale-dependent correction of order β^2, relative to the previous result which ignored nonlinear renormalization effects. Note that the ordinary QCD renormalization effects have been taken into account previously. We thus observe that the prediction of (16) indicates that $(\bar{m}_t)_{max}$ for the ring in Fig. 2b is shifted downward by a factor of β^{-1}, while the $B - \bar{B}$ mixing band is shifted downward by the same factor according to (17) and (18). Hence the non-overlap of the KM annulus and $B - \bar{B}$ mixing band shown in Fig. 2b is not improved by taking the nonlinear renormalization effects into account.

The research of C.H.A. was supported in part by Grant No. PHY-8704240 from the National Science Foundation. Fermilab is operated by Universities Research Association, Inc. under contract with the United States Department of Energy.

REFERENCES

[1] M. Kobayashi and T. Maskawa, Prog. Theor. Phys. 49 (1973) 652.

[2] H. Fritzsch, Phys. Lett. 70B (1977) 436; 73B (1978) 317; 186B (1986) 423.

[3] C. H. Albright and M. Lindner, in preparation.

[4] B. Grzadkowski and M. Lindner, Phys. Lett. B193 (1987) 71.

[5] K. R. Schubert, in Proceedings of the 1987 EPS Conference (Uppsala, 1987).

[6] J. Gasser and H. Leutwyler, Phys. Rep. 87 (1982) 77.

[7] C. Jarlskog and A. Kleppe, Nucl. Phys. B286 (1987) 245; C. Jarlskog, Phys. Rev. D35 (1987) 1685; ibid., D36 (1987) 2138.

[8] C. H. Albright, C. Jarlskog and B.-Å. Lindholm, Phys. Lett. 199B (1987) 553; Phys. Rev. D, to be published.

[9] ARGUS Collaboration (H. Albrecht et al.), Phys. Lett. 192B (1987) 245; and in Proc. of 1987 Intl. Symp. on Lepton and Photon Interactions at High Energies (DESY, Hamburg, 1987).

Fig. 2a. The geometric solution of the allowed range of top masses for the most interesting case where $\bar{\epsilon}_{23} = .022$ is at the lower end of the allowed range, i.e., $m_s = 120MeV$. The ring indicates the possible area for U_{23}. Every triangle with the third upper point inside this area is a solution. The top quark mass is found by mapping the relevant side of the triangle on the horizontal axis, which is labeled with a top mass scale. The angle Φ_B is read off directly.

Fig. 2b. If the data of Fig. 2a are shown in a Φ_B versus m_t plot, the simple geometric interpretaion gets lost. The ring becomes asymmetric and deformed. Additionally, the allowed area from $B - \bar{B}$ mixing is shown. No overlap of the two areas occurs, and the question arises whether nonlinear renormalization effects will change this situation.

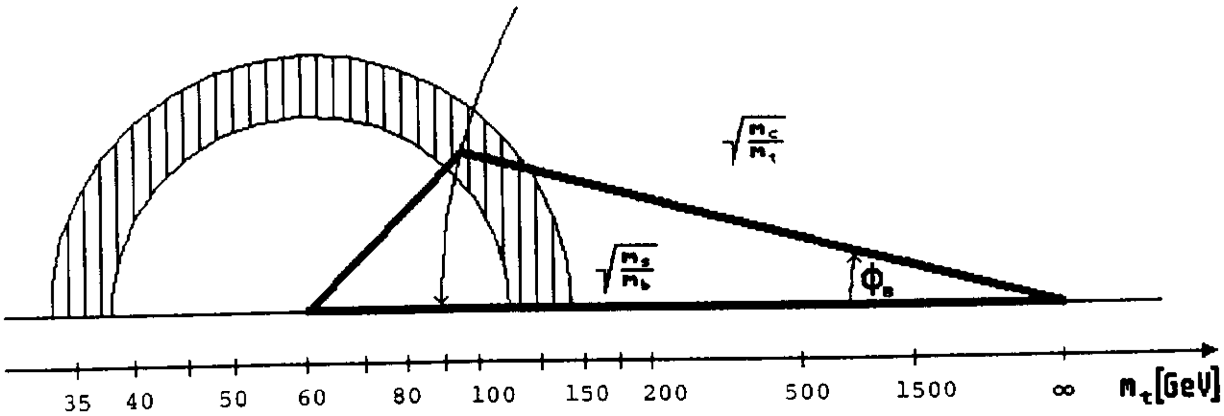

$\sqrt{\frac{m_c}{m_t}}$
$\sqrt{\frac{m_s}{m_b}}$
ϕ_B
35
40
50
60
80
100
150
200
500
1500
∞
m_t[GeV]

Fig. 2a

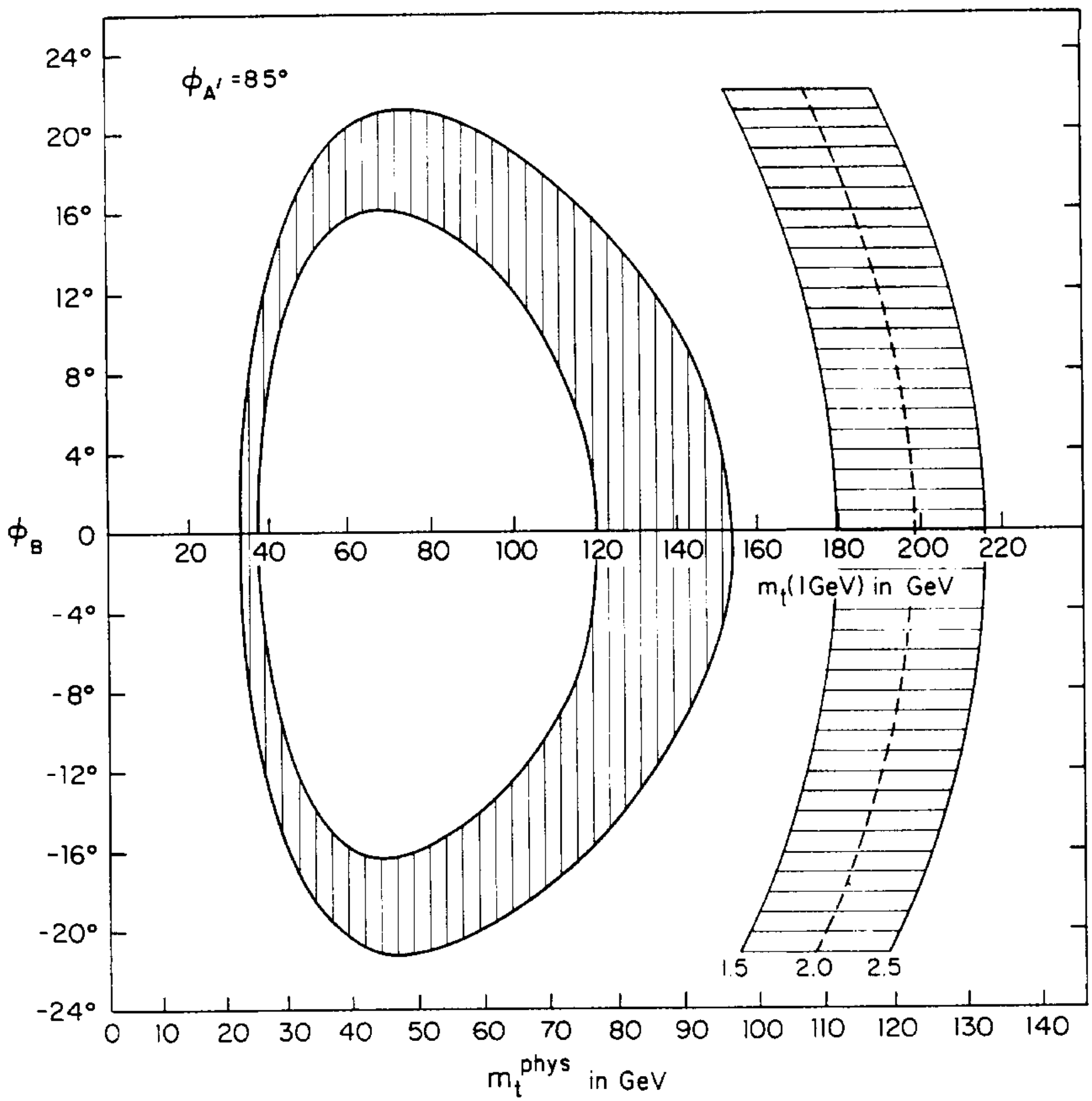

$\phi_{A'} = 85°$
24°
20°
16°
12°
8°
4°
ϕ_B 0
-4°
-8°
-12°
-16°
-20°
-24°
20 40 60 80 100 120 140 160 180 200 220
m_t(1GeV) in GeV
1.5 2.0 2.5
0 10 20 30 40 50 60 70 80 90 100 110 120 130 140
m_t^{phys} in GeV

Fig. 2b